THE JOURNAL OF
PHYSICAL CHEMISTRY A

Article

pubs.acs.org/JPCA

Effects of Heteroatoms of Tetracene and Pentacene Derivatives on Their Stability and Singlet Fission

Yuhan Chen, Li Shen, and Xiyou Li*

Key Laboratory of Colloid and Interface Chemistry, Ministration of Education, Department of Chemistry, Shandong University, Shandong, China, 250100

Ⓢ *Supporting Information*

ABSTRACT: The effects of the introduction of an sp^2-hybridized nitrogen atom (=N—) and thiophene ring on the structure geometries, frontier molecular orbital energies, and excited state energies related to singlet fission (SF) for some tetracene and pentacene derivatives were theoretically investigated by quantum chemical methods. The introduction of a nitrogen atom significantly decreases the energies of frontier molecular orbitals and hence improves their stabilities in air and light illumination. More importantly, it is helpful for reducing the energy loss of the exothermic singlet fission of pentacene derivatives. For fused benzene-thiophene structures, the (α, β) connection pattern could stabilize the frontier molecular orbitals, while the (β, β) connection pattern can promote the thermodynamic driving force of singlet fission. These facts provide a theoretical ground for rational design of SF materials.

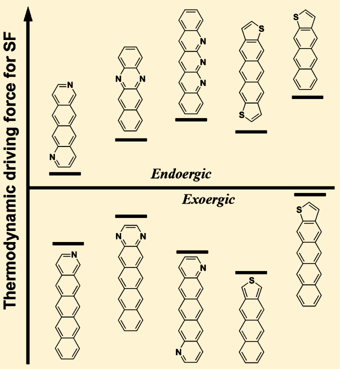

■ INTRODUCTION

Singlet fission (SF), a special case of internal conversion in which a singlet exciton and its ground state neighbor share energy to produce two coupled triplet excited species through a multiexcitonic intermediate state,[1] has recently attracted much attention due to its possibility of overcoming the Shockley—Queisser efficiency limit in conventional photovoltaic cells and increasing the photoelectric transformation efficiency up to 46% theoretically.[2] This process can be very fast, usually in the subpicosecond or picosecond time scale, particularly in molecular crystals.[1] Singlet fission was first invoked to explain the fluorescence quenching in crystalline anthracene in 1965.[3] Since then, triplet states produced by SF have been observed in many compounds, such as tetracene,[4] pentacene,[5] benzophenone,[6] carotenoids,[7,8] conjugated polymers,[9] 5,12-diphenyltetracene (DPT),[10] and rubrene.[11]

Michl and co-workers have explored the energy level matching conditions of SF. First of all, the energy of singlet excited state ($E(S_1)$) must be equal or greater than the twice of the energy of the triplet excited state ($2E(T_1)$) to ensure that the splitting of a singlet exciton into two triplet excitons is thermodynamically possible.[1,12] The energy difference ($2E(T_1) - E(S_1)$), called thermodynamic driving force (ΔE_{SF}) for SF, is regarded strongly impacting the SF yield. Usually, an slight exoergic value for ΔE_{SF} is desirable for a high yield of SF because the SF process must compete effectively with radiative and nonradiative deactivation pathways, but excessive exoergicity would waste much energy and loss of solar cell efficiency.[13] Second, in order to suppress the recombination process of triplet excitons, the energy of the second triplet state ($E(T_2)$) should be equal or greater than $2E(T_1)$.[1,12] It is also expected that T_2 should lie above S_1 to reduce the possibility of undesired fast intersystem crossing (ISC) from S_1 into the triplet manifold.[12]

Two kinds of compounds, alternate hydrocarbons and diradicaloids, have been proposed to be suitable for SF investigation.[1,12] Among them, tetracene and pentacene have been extensively and thoroughly studied because they are recognized as the most promising compounds for SF due to the high yields of triplet states.[4,5] However, the annoying problem is that these acene-based materials degrade easily in the presence of light and air due to the photooxidation.[14,15] This photooxidation, which is commonly found for polycyclic aromatic hydrocarbons (PAHs), could happen in two ways (Figure 1):[16,17] (1) The electron transfer from PAHs to the triplet oxygen ($^3O_2$) leads to the formation of cationic hydrocarbon and highly reactive anionic oxygen, then they interact with each other causing a degradation of PAHs. (2) The photoexcited PAHs could change into triplet state through intersystem crossing and result in highly reactive singlet oxygen

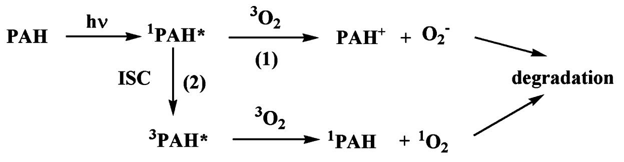

Figure 1. Photooxidation pathways for PAHs: (1) electron transfer (2) singlet oxygen sensitization.[20]

Received: March 28, 2014
Revised: July 4, 2014
Published: July 9, 2014

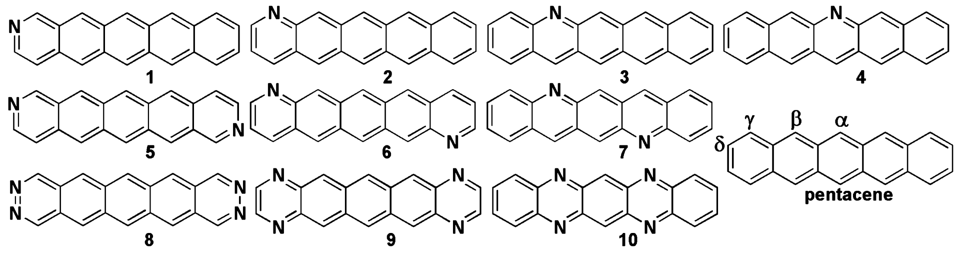

Figure 2. Structures of pentacene and nitrogen-containing pentacene derivatives.

($^1O_2$) by means of oxygen sensitization. Then, the singlet oxygen interacts with the PAHs leading to degradation.

Previous investigation for pentacene degradation indicates that lower energy of the lowest unoccupied molecular orbital (LUMO) could hinder the photooxidation by reducing the rate of electron transfer from the photoexcited PAHs to the triplet oxygen.[18] Additionally, the reduction of the triplet energy of PAHs could prevent $^1O_2$ sensitization because singlet oxygen sensitization requires a larger PAHs triplet excitation energy than the singlet−triplet energy gap in oxygen (0.98 eV[19,20]). Miller et al. also noticed that lower energy of the highest occupied molecular orbital (HOMO) could reduce singlet oxygen sensitization.[21] Though the degradation mechanism is complicated, low HOMO and LUMO energies and small triplet excitation energies are expected to be beneficial to increase the photostability of PAHs.[18−21]

Functionalization of organic molecules is used as a strategy to change the solubility and photostability.[22−26] Miller and co-workers have studied the photooxidative resistances of a series of pentacene derivatives as a function of substituents.[21] Swager has proposed that tetracene with halogen substituents could tune the solubilities in common organic solvents.[22] Introduction of different substitutents can also change the excited-state energy levels[26] and thus tuning the energy difference between the lowest singlet state and twice the lowest triplet state ($2E(T_1) - E(S_1)$). Substituted acenes have been scrutinized experimentally and theoretically, but few studies investigated systematically on singlet fission of heterocyclic derivatives.[12,13] The introduction of heteroatoms offers numbers of opportunities to influence the molecular electronic and optical properties, stabilities toward oxygen and light, solubilities in conventional organic solvents.[27] Considering the fact that *N*-heteroacenes[28,29] and thiophene-based materials[30−32] exhibit unique and excellent electronic and optical properties, we choose sp^2-hybridized nitrogen-containing tetracene and pentacene derivatives, as well the thiophene-containing tetracene and pentacene derivatives as the subject. This study ignores the intermolecular interactions and just focuses on the energy diagram of single molecule. The effects of the introduction, position and number of sp^2-hybridized nitrogen atom and thiophene ring on the energies of frontier molecular orbitals and excited states were systematically investigated.

■ COMPUTATIONAL DETAILS

Density functional theory (DFT) using B3LYP hybrid functional is widely employed in geometrical optimization and has produced a vast number of remarkably accurate results over the past decades.[19,28,29] So the geometries of all the studied molecules were optimized by the B3LYP functional coupled with 6-31G* basis set. The double-ζ quality AO basis set, 6-31G*, is flexible enough to describe the molecular structures.[27,33] The vibrational frequencies calculated at the same level of theory were employed to testify whether the optimized structures were stable geometries.

The frontier molecular orbital energies were evaluated at B3LYP/6-31G* level and the associated HOMO−LUMO gaps can be obtained. The calculated HOMO−LUMO gap for pentacene is 2.211 eV which is in good agreement with the experimental value, 2.14 eV.[34,35] When the basis set enlarges from 6-31G* to 6-311+G**, the calculated results did not show obvious improvement on accuracy. The overall HOMO−LUMO gaps are largely independent of the basis set size.[27] Several molecules were chosen randomly to confirm the above point, and the results are shown in the Supporting Information (Table S1). Therefore, basis set 6-31G* was finally used in the calculation of frontier molecular orbital energies.

The geometries of the singlet ground states (S_0) and the first triplet excited states (T_1) were optimized at the B3LYP/6-31G* level of density functional theory (DFT). Using the relaxed geometries of the corresponding triplet excited states, we obtained the final estimates for adiabatic triplet excitation energies. The spin contamination effect on triplet excitation states is negligibly small because the calculated values of the spin operator $\langle S^2 \rangle$ are extremely close to 2 (Supporting Information Table S2).[36] Hence, the B3LYP/6-31G* method is adequate for describing the triplet excited states. The vertical excitation energies of the first singlet excited states of all the molecules were calculated by time-dependent density functional theory (TDDFT) at the same level. To get the adiabatic excitation energies, the geometries of the excited singlet states were completely optimized with the TDDFT method using B3LYP functional at 6-31G* level. All the calculations were performed with Gaussian 09 program package.[37] The calculated energies for S_1 and T_1 were used to calculate the thermodynamic driving force of SF and thus could theoretically evaluate the singlet fission capability of these molecules based on the energy criterion. The reliability of our calculations is confirmed by the consistency between the theoretical and experimental excitation energies. For example, the computed vertical excitation energy for pentacene, 1.944 eV (the value obtained with the triple-ζ set is 1.899 eV[27]), is in excellent agreement with the corresponding experimental value, 2.14 eV,[34,35] as is known that the TDDFT results often reproduce excitation energies with around 0.2 eV errors.[18,19] The calculated adiabatic excitation energy of the first triplet state for pentacene, 0.775 eV, is also very close to the experimental value, 0.78 eV.[18] Moreover, the computed energy values of these studied heterocyclic molecules agree well with the available theoretical data.[19,20,27] These results indicate that the B3LYP/6-31G* method with low computational cost and high reliability is suitable for rapidly evaluating the energies of frontier molecular orbitals and excited states, and providing a qualitative assessment of photooxidative resistances and the SF efficiency for these series of heterocyclic derivatives.

RESULTS AND DISCUSSION

All the molecular geometries of the proposed models optimized at B3LYP/6-31G* level exhibit planar and rigid skeletons. To clarify the effects of the sp^2-hybridized nitrogen atom and thiophene ring on the energies of the frontier molecular orbitals and excited states of the studied molecules, the calculated results of tetracene and pentacene without heteroatoms are also shown.

Nitrogen-Containing Pentacene Derivatives. *Stability Reflected by the Frontier Molecular Orbital Energies.* The molecular structures of these nitrogen-containing derivatives are shown in Figure S1. They are the results of successive replacement of C−H groups by nitrogen atoms at different positions of pentacene. The effects of sp^2-hybridized nitrogen atom on the HOMOs, LUMOs and HOMO−LUMO gaps were systematically investigated and consequently the stabilities of the derivatives can be estimated from these data (Table S3). Figure 2 shows the typical molecules and will be discussed in detail.

The mononitrogen (1N) substituted derivatives, compounds **1**−**4**, with different substitution positions, *δ*, *γ*, *β* and *α*, are shown in the first row of Figure 2. As shown in Figure 3, the introduction of nitrogen atom in pentacene has reduced the energies of both HOMO and LUMO. Along with the position of nitrogen atom changes in the sequence of *α*−*δ*−*β*−*γ*, the HOMO energy increases from −4.906 to −4.756 eV. Meanwhile, the LUMO energy increases gradually in the sequence of *δ*−*α*−*β*−*γ*. Obviously, introducing nitrogen atom at *α* position leads to the lowest HOMO energy among these four molecules, and the lowest LUMO energy can be obtained when N-replacement happened at *δ* position. Due to the nearly same contributions of nitrogen atom to HOMO and LUMO energies, there is little change of the HOMO−LUMO gaps of all these four compounds.

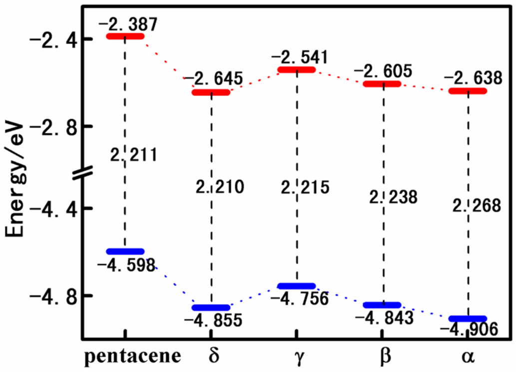

Figure 3. HOMO (blue, bottom) and LUMO (red, upper) energies (eV) of pentacene and monosubstituted nitrogen-containing pentacene derivatives with different substitution positions (*α*, *β*, *γ* and *δ*) obtained at the B3LYP/6-31G* level.

Along with the increase on the nitrogen atom numbers in the pentacene ring, the HOMO (Figure 4a) and LUMO (Figure 4b) energies decrease progressively. Take the series of *δ*-substituted molecules (**1**, **5**, and **8** in Figure 2) as example. In comparison with that of monosubstituted **1**, the frontier molecular orbital energies of disubstituted **5** decrease by 0.266 eV in HOMO and 0.256 eV in LUMO. **8** with four nitrogen atoms has the lowest HOMO and LUMO energies among these three compounds, which decreased by 1.213 and 1.016 eV in HOMO and LUMO, respectively, in comparison with those of pentacene and are three times larger than those of **1**. The same trend is also observed in other series of molecules (series **2**, **6**, and **9** or **3**, **7**, and **10**).

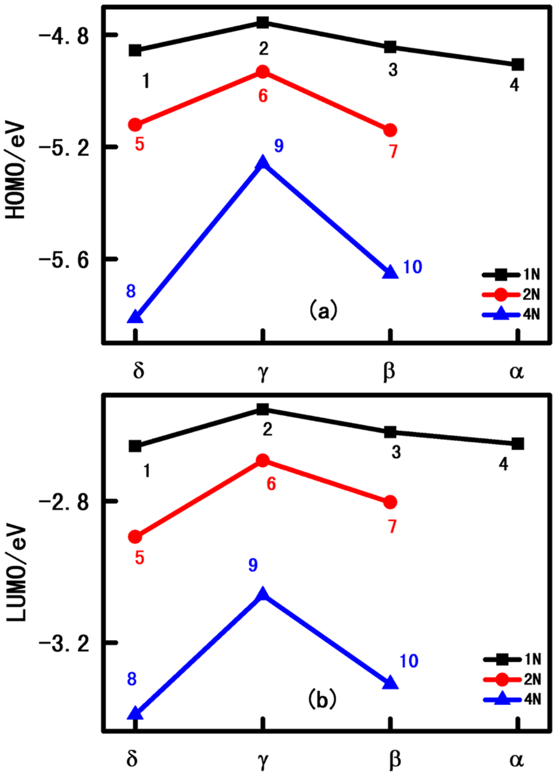

Figure 4. HOMO (a) and LUMO (b) energies (eV) (1N, 2N, and 4N indicate the number of the nitrogen atoms in molecules) of nitrogen-containing pentacene derivatives with different numbers at *α*, *β*, *γ*, and *δ* positions obtained at the B3LYP/6-31G* level.

Figure 4 also indicates that introducing more nitrogen atoms could magnify the effects of the substitution position on frontier molecular orbital energies. For monosubstituted molecules, *δ*-substituted **1** and *β*-substituted **3** have almost the same HOMO and LUMO energies with a small difference of 0.012 and 0.04 eV. However, for disubstituted compounds, the difference between LUMOs of **5** and **7** rises to 0.1 eV. This has also been supported by the extra high HOMO and LUMO energies of compound **9**. Clearly, the ability of reducing the frontier molecular orbital energies is roughly in the order $\alpha > \delta > \beta > \gamma$, and the increase on the number of nitrogen atoms will amplify the effects of nitrogen atoms on reducing the energies of frontier molecular orbitals.

In general, not only the position but also the number of nitrogen atoms can significantly influence the frontier orbital energies and consequently influence the HOMO−LUMO gaps. It is well-known that nitrogen atom possesses strong electron-withdrawing ability,[28] so there is no surprise that the introduction of the sp^2-hybridized nitrogen atom could stabilize the frontier molecular orbitals due to the strong inductive effect.[21,26] With the increase of the nitrogen atom numbers in the pentacene ring, the effect of nitrogen atoms on reducing the energies of HOMO and LUMO became more and more significant, which may attribute to the accumulated inductive effects caused by the strong electronegativity of nitrogen atoms.[26]

The calculated linear combination of atomic orbital (LCAO) coefficients of the HOMO and LUMO for pentacene indicate that the LCAO coefficients increase in the order $\gamma < \delta \ll \beta < \alpha$.[26] Previous works demonstrated that the larger the LCAO coefficient is, the more the frontier molecular orbitals are stabilized by the inductive effect.[26] Obviously, the HOMO and LUMO energies of γ, β, and α substituted compounds are stabilized following this order due to the same increasing order for the inductive effects. But the δ position substituted compounds show exceptional stabilized HOMO and LUMO energies, which can be ascribed to the unique electronic nature of this position.[38] The inductive effect caused by the substituents at this position are also very sensitive to the nature of the substituents.[26,38] Thus, the extra large inductive effect of the nitrogen atoms at δ position is possible.

Thermodynamic Driving Force for SF Yield. For efficient formation of triplet states by SF, the condition $E(S_1) \geq 2E(T_1)$ should be satisfied to ensure the process of SF slightly exoergic or at least isoergic. Usually, the value of ΔE_{SF} $(2E(T_1) - E(S_1))$ is applied to evaluate the yield of SF.[12] The process of singlet fission in pentacene crystal is exoergic. The question is how the introduction of nitrogen atom changes the ΔE_{SF}. To answer this question, the $E(T_1)$ and $E(S_1)$ of these nitrogen hybridized pentacene derivatives were calculated (Table S4) and the important results are summarized in Figure 5.

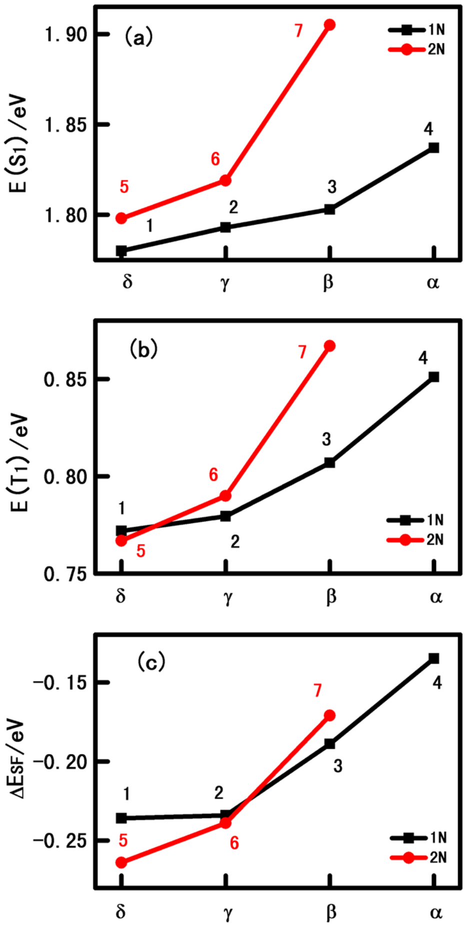

Figure 5. $E(S_1)$ (a), $E(T_1)$ (b), and ΔE_{SF} (c) (1N and 2N indicate the number of the nitrogen atoms in molecules) of nitrogen-containing pentacene derivatives with different numbers of nitrogen atoms at α, β, γ, and δ positions obtained at the B3LYP/6-31G* level.

For γ- and β-substituted molecules, **2** and **3**, the $E(S_1)$ are similar to that of pentacene (1.802 eV), while the $E(T_1)$ are larger than that of pentacene (0.775 eV), leading to the inevitable increase of ΔE_{SF} of **2** and **3** in comparison with that of pentacene (−0.252 eV). For δ- and α-substituted molecules, **1** and **4**, the ΔE_{SF} are also larger than that of parent pentacene, due to $E(T_1)$ increases with a larger extent than $E(S_1)$ does. $E(S_1)$ of monosubstituted molecules increases gradually from 1.780 to 1.837 eV (Figure 5a) when the substitution position changes following the order of δ–γ–β–α. $E(T_1)$ increases in the same order from 0.772 to 0.851 eV (Figure 5b). The values of ΔE_{SF} (Figure 5c) change follow the order of pentacene < **1**(δ) < **2**(γ) < **3**(β) < **4**(α). Obviously, introduction of nitrogen atom increases the ΔE_{SF} of the molecules, but they are still negative and the SF process in these molecules should be exoergic. Considering the ΔE_{SF} of these nitrogen hybridized compounds are more close to zero than pentacene, the energy loss due to the SF process should be small. This is favorable for the application of SF in solar cells.[13]

For the disubstituted molecules **5**, **6**, and **7**, the values of $E(S_1)$, $E(T_1)$, and ΔE_{SF} change follow the same order as the monosubstituted compounds. However, the differences on these values between compounds with different substitution positions have been obviously enlarged, which can be seen clearly from the increased slopes of the connection lines between the points in Figure 5. It is worth mentioning that $E(S_1)$ and $E(T_1)$ for the disubstituted compounds always increase with respect to those of the corresponding monosubstituted compounds except **5**. Compound **5** has a slight smaller $E(T_1)$ than **1**, which can be ascribed to the subtle increase of delocalization of frontier orbitals of **5**, particularly the LUMO (Figure S2, **1**−**1** and **5**−**1**). The effects of the introduction of the second nitrogen atom in these disubstituted compounds on ΔE_{SF} are complicated. Only **7** among these three disubstituted compounds has a larger ΔE_{SF} than its counterpart **3**. The ΔE_{SF} of both **5** and **6** are smaller than that of their counterpart **1** and **2**. It seems that there is no necessary correlation between the larger ΔE_{SF} and the increase of nitrogen atoms. This result can also be testified by other data in Table S4.

Generally, both the position and number, including substitution patterns (Figure S3) of nitrogen atoms can significantly influence $E(S_1)$ and $E(T_1)$, and consequently influence the ΔE_{SF}. It is well-known that the origin of the S_1 and T_1 can be reflected by the HOMO and LUMO frontier molecular orbitals that primarily comprise these states.[39] As shown in Figure S2, introducing nitrogen atoms decreases the wave function delocalization of frontier orbitals, thus increasing the $E(S_1)$ and $E(T_1)$. As a result, ΔE_{SF} increase because they are obtained by double $E(T_1)$ minus $E(S_1)$. Figure S2 also shows that the electron cloud density reaches a maximum in the middle ring of pentacene and decreases gradually from the middle to the terminal. Obviously, the nitrogen atom in the middle ring has a greater influence on electron cloud density than that in the terminal ones. This may be the reason why the $E(S_1)$, $E(T_1)$ and ΔE_{SF} change follow the order of $\alpha > \beta > \gamma > \delta$.

The increase of ΔE_{SF} is beneficial to the SF in compounds having low $E(T_1)$ or much small S_0-T_1 gaps, because the increased $E(T_1)$ can make twice the S_0-T_1 gap tend to the S_1−S_0 gap, reducing the waste of energy and improving the solar cell efficiency.[13] However, it may be adverse to compounds having an endoergic singlet fission process (the $2E(T_1)$ is slightly larger than $E(S_1)$) because the energy deficit (ΔE_{SF}, $2E(T_1) - E(S_1)$) will become larger. This can be testified by some nitrogen-containing tetracene derivatives (Figure S4–S5, Table S5 in the Supporting Information).

We also investigated the relationships between excited state energies and HOMO–LUMO gaps (ΔE) of nitrogen-containing pentacene and tetracene derivatives. The correlations of $E(S_1)$ and $E(T_1)$ with ΔE are studied by regression analysis. As shown in Figure 6, there exist good linear relationships between $E(S_1)$ or $E(T_1)$ and ΔE, with the linear correlation coefficients (R) of 0.986 and 0.980, respectively. When ΔE is smaller than 2.555 eV, $E(S_1)$ is larger than $2E(T_1)$, which means ΔE_{SF} is negative, and the SF is thermaldynamically favorable. When ΔE is larger than 2.555 eV, $E(S_1)$ is smaller than $2E(T_1)$ and SF is thermaldynmically unfavorable. This is consistent with previous work that the smaller ΔE is closely related to larger diradical character, and simultaneously, smaller ΔE_{SF}.[40,41]

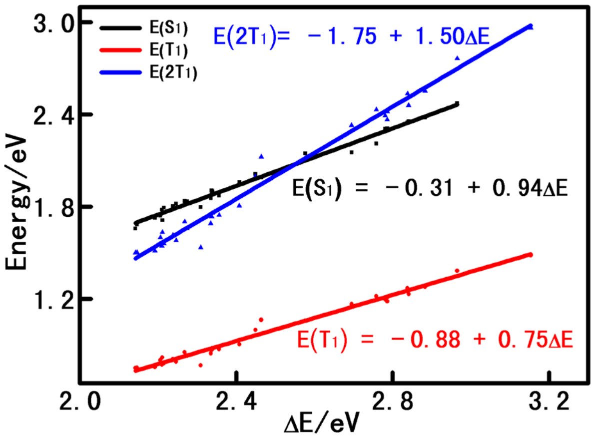

Figure 6. Correlations of $E(S_1)$, $E(T_1)$, and $2E(T_1)$ with the ΔE of nitrogen-containing pentacene and tetracene derivatives.

Thiophene-Containing Tetracene and Pentacene Derivatives. *Stability Reflected by the Frontier Molecular Orbital Energies.* The molecular structures of thiophene-substituted compounds are shown in Figure S6, and some typical ones are shown in Figure 7. These derivatives can be divided into two groups. One group contains compounds like **32** with two β positions of thiophene ring connected with benzene ring (β, β pattern). The other group includes the compounds like **33**, with one α and one β position of thiophene connected with benzene ring (α, β pattern). The HOMOs and LUMOs, as well as the HOMO–LUMO gaps of **31**–**50** are summarized in Table S6.

Compared with tetracene, the HOMO energy of anthra[2,3-*b*]thiophene (**33**) decreases by 0.115 eV, whereas that of anthra[2,3-*c*]thiophene (**32**) increases by more than 0.3 eV (Figure 8). Oppositely, the LUMO energy of **33** is higher than that of tetracene, while the LUMO energy of **32** is smaller than that of tetracene. Hence, the HOMO–LUMO gap of **33** is much larger than that of **32**. Molecular orbital diagram (Figure 9) reveals that sulfur atom in **33** just makes a contribution to HOMO, whereas the contribution to LUMO is zero. But in **32**, the sulfur atom contributes only to LUMO and does not to HOMO. Obviously, the different contribution of sulfur atom to HOMO and LUMO is the reason for the aforementioned differences on the frontier molecular orbital energies of **33** and **32**. These differences are also observed between the thiophene-containing pentacene derivatives, tetraceno[2,3-*b*]thiophene (**37**) and tetraceno[2,3-*c*]thiophene (**36**), indicating that the sulfur atom can significantly change the frontier orbital energies of tetracene and pentacene derivatives (Table S6).

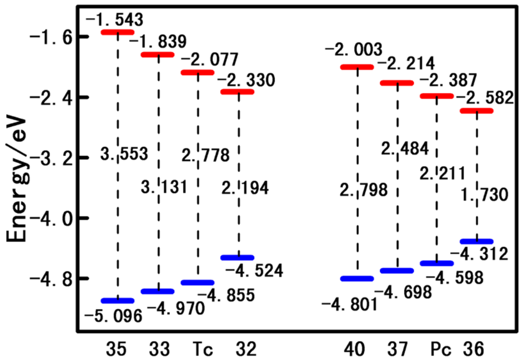

Figure 8. HOMO (blue, bottom) and LUMO (red, upper) energies of tetracene (Tc), pentacene (Pc) and thiophene-substituted molecules **32**, **33**, **35**, **36**, **37**, and **40**.

Figure 8 also shows that when the two terminal benzene rings of tetracene are both replaced by thiophene rings (**35**, in both (α, β pattern)), the HOMO energy decreases by 0.126 eV with respect to that of the one terminal benzene ring replaced compound **33**. Meanwhile, the LUMO energy of **35** increases by 0.286 eV in comparison with that of **33**. Analyzing the distribution of the frontier molecular orbitals of **33** as shown in Figure 9, the HOMO of **33** presents an antibonding character between the carbon and sulfur atoms. **35** with two terminal thiophene rings has inevitably antibonding character at two sites, resulting in the relatively low HOMO energy.[42] The additional nodal plane in the LUMO along the long molecular axis of **35** compared to that of **33** may play an important role in the increase of LUMO energy.

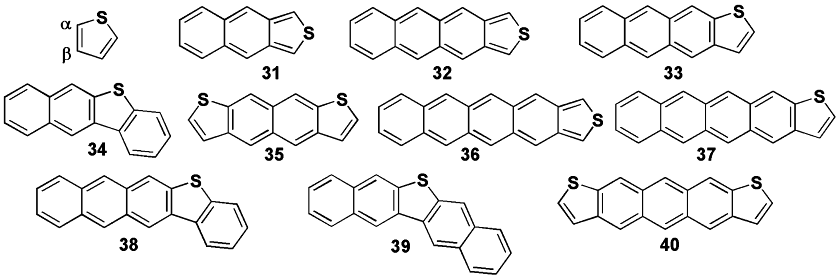

Figure 7. Structures of thiophene and thiophene-containing tetracene and pentacene derivatives.

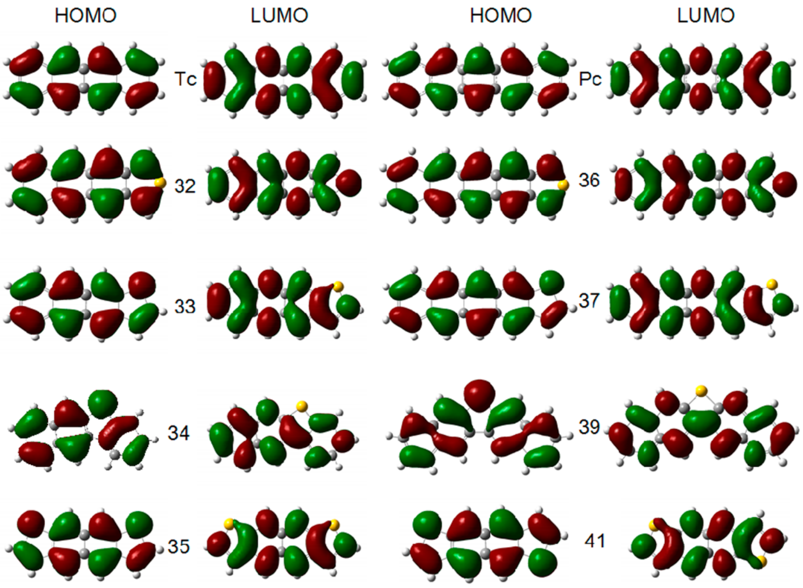

Figure 9. Molecular orbital (isovalue = 0.02) diagram of some thiophene-substituted molecules (**41** is the isomer of **35**, its structure can be seen in the Supporting Information).

When thiophene ring moves from the terminal, **33**, to the middle, **34**, the HOMO energy decreases further to −5.434 eV and the LUMO energy increases to −1.430 eV (Figure 10).

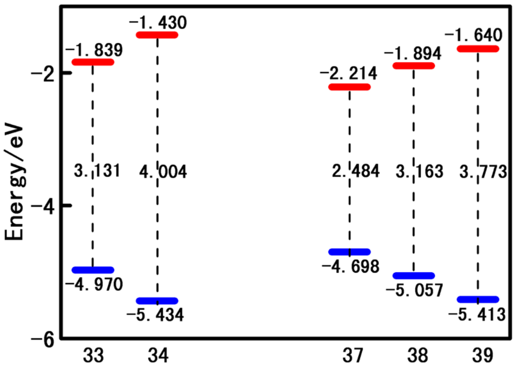

Figure 10. HOMO (blue, bottom) and LUMO (red, upper) energies of thiophene-containing compounds **33**, **34**, **37**, **38**, and **39**.

Molecule **39**, a pentacene derivative contains also a central thiophene ring, has the lowest HOMO and highest LUMO energies among the monothiophene ring containing pentacene derivatives **37**−**39**. Figure 9 shows that the distribution of the frontier molecular orbitals of **34** and **39** is significantly different from that of tetracene or pentacene. As previously mentioned, **39** is a structural analogue of pentaphene rather than pentacene.[42] Hence, there have huge changes on frontier orbital energies.

The calculated results indicate that the introduction of thiophene ring can change the energies of the frontier molecular orbitals significantly. Generally, molecules with (β, β) connected thiophene ring have smaller HOMO−LUMO gaps than those of the corresponding acenes due to the increased HOMO energies and decreased LUMO energies. However, molecules with (α, β) connected thiophene ring have larger HOMO−LUMO gaps because the opposite effects on HOMO and LUMO energies. Previous works have reported that tetraceno[2,3-*b*]thiophene is more stable under ambient conditions than pentacene which may due to its asymmetrical structure and lower HOMO energy than that of pentacene.[33,43] Katz and co-workers have also manifested that anthradithiophene (**40**) displays improved environmental stability toward oxidation with respect to pentacene.[44,45] For the same reason, we believe that molecules with relatively low HOMO energies, like **33**, **37**, and **40**, may be more stable.

Thermodynamic Driving Force for SF. It is well-known that larger diradical character leads to smaller ΔE_{SF},[40,46] and diradical characteristic is closely related to the aromatic characteristics.[47,48] Thiophene, a five membered heterocyclic molecule containing four carbon atoms and one sulfur atom, is considered to be aromatic because of the significantly delocalized electron pairs of sulfur on the conjugated π system.[49] Because replacing benzene ring with thiophene ring could influence the diradical character of molecules,[47] it is expected that thiophene ring will show large effect on the SF process. In this section, the energy difference between $2E(T_1)$ and $E(S_1)$, which is known as thermodynamic driving force for SF, is calculated and also used to evaluate the singlet fission capabilities of these molecules. The calculated excitation energies of the first excited singlet and the first excited triplet of the designed molecules are collected in Table S7.

It can be seen in Figure 11 that compounds **31** and **32** meet the condition: $E(S_1) > 2E(T_1)$ ($\Delta E_{SF} < 0$). This indicates that the introduction of thiophene (connected in (β, β pattern)) has reduced the ΔE_{SF}, which is beneficial to singlet fission of anthracene and tetracene deravitives because the parent anthracene and tetracene have positive ΔE_{SF}. The values of ΔE_{SF} decrease along with the increase of the number of benzene rings in series of **31**, **32**, and **36** due to the expanded conjugated network.[41]

When the connection position of thiophene ring is changed from (β, β) pattern to (α, β) pattern, dramatic changes on ΔE_{SF} can be observed. For **33** ((α, β) pattern), the condition $E(S_1) > 2E(T_1)$ is broken because of the large value of $E(T_1)$ (1.543 eV) (Figure 12), therefore, the SF of **33** is thermodynamically unfavorable. Molecular orbital diagram reveals that sulfur atom in **33** makes no contribution to LUMO, resulting in the

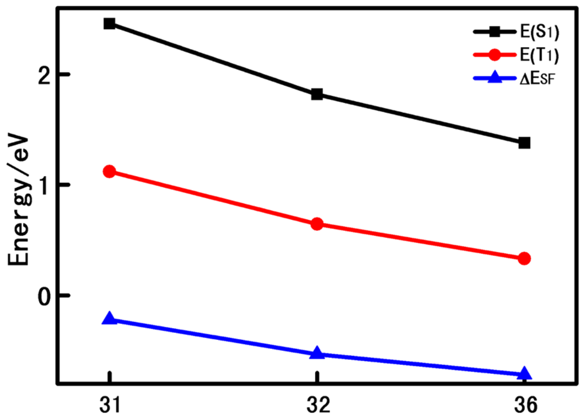

Figure 11. Calculated excitation energies and thermodynamic driving force (eV) for **31**, **32**, and **36** obtained at B3LYP/6-31G* level.

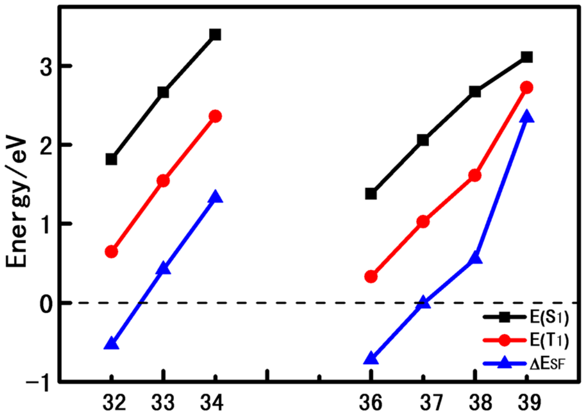

Figure 12. Calculated excitation energies and thermodynamic driving force (eV) for different series of thiophene-introduced molecules obtained at B3LYP/6-31G* level.

decreased delocalization of electrons. This may be the reason for the relative large $E(T_1)$ of **33**. Similarly, significant difference on ΔE_{SF} caused by the connection pattern of thiophene ring has also been observed between **36** and **37**. The ΔE_{SF} of **36** (thiophene ring connected in (β, β) pattern) is much smaller than that of **37** (thiophene ring connected in (α, β) pattern). The large negative ΔE_{SF} for **36** provides a large driving force for SF, but also a large energy loss. Therefore, it is not favorable for the application of SF in solar cells.[12,13] The best SF materials for a solar cell should have a small negative ΔE_{SF}, which could ensure a thermodynamically favorable SF and minimize energy loss during SF. It is exciting that the ΔE_{SF} of **37** is only −0.010 eV which is negative but very close to zero, and hence meet the requirements of a good SF molecule.

When the thiophene ring was moved from the terminal, **33**, to the middle, **34**, both $E(S_1)$ and $E(T_1)$ increased obviously (Figure 12). The ΔE_{SF} of **34** increased by 0.905 eV with respect to that of **33** (0.421 eV). Molecule **39**, a pentacene derivative containing a central thiophene ring, has the largest $E(S_1)$, $E(T_1)$ and ΔE_{SF} in the monothiophene containing compounds **37**–**39**. According to the previous research, **39** is no longer the structural analogue of pentacene but an analogue of pentaphene due to the replacement of middle benzene ring by thiophene.[42] Along the axis of a specific direction, the length of conjugated chain of **39** (pentaphene with 14 carbon atoms) is too short to meet the basic condition of SF, as is known that the first condition of an efficient SF is not filled until the π-system of alternant hydrocarbons contains about 20 carbon atoms.[13] Other molecules with thiophene ring connected in the middle of the molecule have also large positive ΔE_{SF} and can be ascribed to the same reason.

It is reported that a small HOMO−LUMO gap (ΔE) could enhance the diradical character,[40] and the energies of S_1 and T_1 could be influenced by the diradical character.[41] So we also investigated the relationships between excited state energies and ΔE of thiophene-containing molecules. The correlations of $E(S_1)$ and $E(T_1)$ with ΔE are studied by regression analysis. As shown in Figure 13, there exist good linear relationships between $E(S_1)$ or $E(T_1)$ and ΔE, with the linear correlation coefficients (R) of 0.997 and 0.956, respectively. From the slopes of the regression equations, $E(S_1)$ increases more rapidly than $E(T_1)$ along with the increase of ΔE. When ΔE is smaller than 2.596 eV, $E(S_1)$ is larger than $2E(T_1)$, which means ΔE_{SF} is negative, and the SF is thermodynamically favorable. When ΔE is larger than 2.596 eV, $E(S_1)$ is smaller than $2E(T_1)$ and SF is thermodynamically unfavorable. This is consistent with previous work that the smaller ΔE is closely related to larger diradical character, and simultaneously, smaller ΔE_{SF}.[40,41]

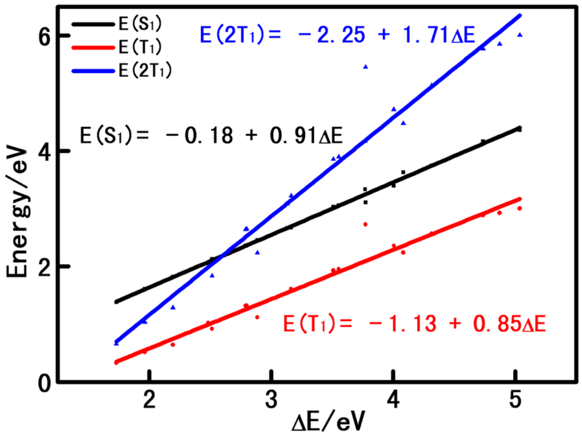

Figure 13. Correlations of $E(S_1)$, $E(T_1)$, and $2E(T_1)$ with the ΔE.

In conclusion, the introduction of thiophene ring can strongly affect the excited state energies of S_1 and T_1 due to the large effect on electron delocalization in the conjugated π system. For fused benzene-thiophene structures, thiophene ring in (β, β) connection pattern could give full play to its ability of delocalization, thus improving the diradical character of molecules and finally improving the thermodynamic driving force of singlet fission. However, thiophene ring in (α, β) connection pattern can dramatically increase the ΔE_{SF} and lead to an endothermic SF. This is consistent with the previous work.[47]

■ CONCLUSIONS

A number of sp^2-hybridized nitrogen-substituted pentacene derivatives and thiophene-fused acenes have been investigated theoretically to elucidate the effects of heteroatoms of tetracene and pentacene rings on their stabilities and singlet fission abilities. Introducing nitrogen atom helps to decrease the frontier orbital energies, especially when the N-replacement happened at α and δ positions. The HOMO and LUMO energies continuously decrease with the increase of nitrogen atoms. The introduction of sp^2-hybridized nitrogen atoms can also effectively increase the ΔE_{SF}. For the molecules with an exothermic SF, such as pentacene, this increase of ΔE_{SF} will reduce the energy loss of singlet fission, and therefore, it is favorable for the application of SF in solar cells. However, for the molecules with an endothermic SF, such as tetracene, this increase on ΔE_{SF} will lead to a thermodynamically unfavorable SF.

For fused benzene-thiophene molecules, the frontier orbital energies and the excited energies are largely influenced by position, number, and connection patterns $((\alpha, \beta)$ and $(\beta, \beta))$ of thiophene ring. Thiophene ring condensed with benzene ring in (α, β) pattern usually decreases the HOMO energy and increases the LUMO energy, resulting in a large HOMO−LUMO gap and positive ΔE_{SF}, which is harmful for SF. However, thiophene ring condensed with benzene ring in (β, β) connection pattern usually increases the HOMO energy and decreases the LUMO energy, resulting in a small HOMO−LUMO gap. This connection pattern could also enhance the diradical character of molecules and benefit the SF process. **37** which has already been synthesized[43] may be the best candidate for SF due to the high solubility, stability and high SF efficiency. **32** and **36** with high diradical characters need further modification due to the small T_1 values[13,41] and instabilities.

■ ASSOCIATED CONTENT

Ⓢ Supporting Information

Comparisons of HOMOs, LUMOs, and HOMO−LUMO gaps of molecules with different basis sets at B3LYP level. $\langle S^2 \rangle$ values for Tn (n = 1, 2) states of the 50 compounds obtained at the B3LYP/6-31G* level. Molecular structures, molecular orbital diagram (including nitrogen-containing tetracene derivatives), frontier molecular orbital energies, and excited state energies of nitrogen-containing pentacene derivatives. Molecular structures, energies of frontier molecular orbitals, and excited states of nitrogen-containing tetracene derivatives. Molecular structures, energies of frontier molecular orbitals, and excited states of thiophene-containing tetracene and pentacene derivatives. Full author list for ref 37. This material is available free of charge via the Internet at http://pubs.acs.org.

■ AUTHOR INFORMATION

Corresponding Author

*E-mail: xiyouli@sdu.edu.cn. Phone: +86-531-88369877. Fax: +86-531-88564464.

Notes

The authors declare no competing financial interest.

■ ACKNOWLEDGMENTS

We thank the Natural Science Foundation of China (with Grant Nos. 21073112, 91233108, and 21173136) and the National Basic Research Program of China (973 Program: 2012CB93280) for the financial support.

■ REFERENCES

(1) Smith, M. B.; Michl, J. Singlet Fission. *Chem. Rev.* **2010**, *110*, 6891−6936.

(2) Shockley, W.; Queisser, H. J. Detailed Balance Limit of Efficiency of p-n Junction Solar Cells. *J. Appl. Phys.* **1961**, *32*, 510−519.

(3) Singh, S.; Jones, W. J.; Siebrand, W.; Stoicheff, B. P.; Schneider, W. G. Laser Generation of Excitons and Fluorescence in Anthracene Crystals. *J. Chem. Phys.* **1965**, *42*, 330−342.

(4) Burdett, J. J.; Müller, A. M.; Gosztola, D.; Bardeen, C. J. Excited State Dynamics in Solid and Monomeric Tetracene: the Roles of Superradiance and Exciton Fission. *J. Chem. Phys.* **2010**, *133*, 144506/1−144506/12.

(5) Chason, M.; Brazis, P. W. J.; Zhang, J.; Kalyanasundaram, K.; Gamota, D. R. Printed Organic Semiconducting Devices. *Proc. IEEE* **2005**, *93*, 1348−1356.

(6) Katoh, R.; Kotani, M.; Hirata, Y.; Okada, T. Triplet Exciton Formation in a Benzophenone Single Crystal Studied by Picosecond Time-Resolved Absorption Spectroscopy. *Chem. Phys. Lett.* **1997**, *264*, 631−635.

(7) Rademaker, H.; Hoff, A. J.; Grondelle, R.; Duysens, L. N. Carotenoid Triplet Yields in Normal and Deuterated Rhodospirillum Rubrum. *Biochim. Biophys. Acta* **1980**, *592*, 240−257.

(8) Papagiannakis, E.; Das, S. K.; Gall, A.; Stokkum, I. H. V.; Robert, B.; Grondelle, R.; Frank, H. A.; Kennis, J. T. M. Light Harvesting by Carotenoids Incorporated into the B850 Light-Harvesting Complex from Rhodobacter Sphaeroides R-26.1: Excited-State Relaxation, Ultrafast Triplet Formation, and Energy Transfer to Bacteriochlorophyll. *J. Phys. Chem. B* **2003**, *107*, 5642−5649.

(9) Austin, R. H.; Baker, G. L.; Etemad, S.; Thompson, R. Magnetic Field Effects on Triplet Exciton Fission and Fusion in a Polydiacetylene. *J. Chem. Phys.* **1989**, *90*, 6642−6646.

(10) Roberts, S. T.; McAnally, R. E.; Mastron, J. N.; Webber, D. H.; Whited, M. T.; Brutchey, R. L.; Thompson, M. E.; Bradforth, S. E. Efficient Singlet Fission Discovered in a Disordered Acene Film. *J. Am. Chem. Soc.* **2012**, *134*, 6388−6400.

(11) Reusswig, P. D.; Congreve, D. N.; Thompson, N. J.; Baldo, M. A. Enhanced External Quantum Efficiency in an Organic Photovoltaic Cell via Singlet Fission Exciton Sensitizer. *Appl. Phys. Lett.* **2012**, *101*, 113304/1−113304/4.

(12) Paci, I.; Johnson, J. C.; Chen, X.; Rana, G.; Popovic, D.; David, D. E.; Nojik, A. J.; Ratner, M. A.; Michl, J. Singlet Fission for Dye-Sensitized Solar Cells: Can a Suitable Sensitizer Be Found ? *J. Am. Chem. Soc.* **2006**, *128*, 16546−16553.

(13) Akdag, A.; Havlas, Z.; Michl, J. Search for a Small Chromophore with Efficient Singlet Fission: Biradicaloid Heterocycles. *J. Am. Chem. Soc.* **2012**, *134*, 14624−14631.

(14) Liang, Z.; Zhao, W.; Wang, S.; Tang, Q.; Lam, S. C.; Miao, Q. Unexpected Photooxidation of H-Bonded Tetracene. *Org. Lett.* **2008**, *10*, 2007−2010.

(15) Yamada, M.; Ikemoto, I.; Kuroda, H. Photooxidation of the Evaporated Films of Polycyclic Aromatic Hydrocarbons Studied by X-Ray Photoelectron Spectroscopy. *Bull. Chem. Soc. Jpn.* **1988**, *61*, 1057−1062.

(16) Stevens, B.; Perez, S. R.; Ors, J. A. Photoperoxidation of Unsaturated Organic Molecules. XIV. O21.DELTA.g Acceptor Properties and Reactivity. *J. Am. Chem. Soc.* **1974**, *96*, 6846−6850.

(17) Mazur, M.; Blanchard, G. J. Photochemical and Electrochemical Oxidation Reactions of Surface-Bound Polycyclic Aromatic Hydrocarbons. *J. Phys. Chem. B* **2004**, *108*, 1038−1045.

(18) Maliakal, A.; Raghavachari, K.; Katz, H.; Chandross, E.; Siegrist, T. Photochemical Stability of Pentacene and a Substituted Pentacene in Solution and in Thin Films. *Chem. Mater.* **2004**, *16*, 4980−4986.

(19) Sundaram, A.; Takahisa, O. Attractive Tetraceno[2,3-b]-thiophene Derivatives for Organic Transistor Applications: A Theoretical Analysis. *J. Phys. Chem. C* **2008**, *112*, 16561−16567.

(20) Zhao, C.; Wang, W. L.; Ma, Y. Molecular Design Toward Good Hole Transport Materials Based on Anthra[2,3-c]thiophene: A Theoretical Investigation. *Comput. Theor. Chem.* **2013**, *1010*, 25−31.

(21) Kaur, I.; Jia, W.; Kopreski, R. P.; Selvarasah, S.; Dokmeci, M. R.; Pramanik, C.; McGruer, N. E.; Miller, G. P. Substituent Effects in Pentacenes: Gaining Control over HOMO-LUMO Gaps and Photooxidative Resistances. *J. Am. Chem. Soc.* **2008**, *130*, 16274−16286.

(22) Chen, Z.; Müller, P.; Swager, T. M. Syntheses of Soluble, π-Stacking Tetracene Derivatives. *Org. Lett.* **2006**, *8*, 273−276.

(23) Katsuta, S.; Miyagi, D.; Yamada, H.; Okujima, T.; Mori, S.; Nakayama, K.; Uno, H. Synthesis, Properties, and Ambipolar Organic Field-Effect Transistor Performances of Symmetrically Cyanated

Pentacene and Naphthacene as Air-Stable Acene Derivatives. *Org. Lett.* **2011**, *13*, 1454−1457.

(24) Ono, K.; Totani, H.; Hiei, T.; Yoshino, A.; Saito, K.; Eguchi, K.; Tomura, M.; Nishida, J.; Yamashita, Y. Synthesis, Properties, and Photoreaction of Pentacene Derivatives Substituted by Aromatic Groups. *Tetrahedron.* **2007**, *63*, 9699−9704.

(25) Kaur, I.; Stein, N. N.; Kopreski, R. P.; Miller, G. P. Exploiting Substituent Effects for the Synthesis of a Photooxidatively Resistant Heptacene Derivative. *J. Am. Chem. Soc.* **2009**, *131*, 3424−3425.

(26) Medina, B. C. M.; Anthony, J. E.; Gierschner, J. Independent Tuning of Electronic Levels in Pentacene by Site-Specific Substitution. *ChemPhysChem* **2008**, *9*, 1519−1523.

(27) Winkler, M.; Houk, K. N. Nitrogen-Rich Oligoacenes: Candidates for n-Channel Organic Semiconductors. *J. Am. Chem. Soc.* **2007**, *129*, 1805−1815.

(28) Chen, X. K.; Guo, J. F.; Zou, L. Y.; Ren, A. M.; Fan, J. X. A Promising Approach to Obtain Excellentn-Type Organic Field-Effect Transistors: Introducing Pyrazine Ring. *J. Phys. Chem. C* **2011**, *115*, 21416−21428.

(29) Chen, H.; Chao, I. Toward the Rational Design of Functionalized Pentacenes: Reduction of the Impact of Functionalization on the Reorganization Energy. *ChemPhysChem.* **2006**, *7*, 2003−2007.

(30) Liang, Y. Y.; Xu, Z.; Xia, J. B.; Tsai, S. T.; Wu, Y.; Li, G.; Ray, C.; Yu, L. P. For the Bright Future—Bulk Heterojunction Polymer Solar Cells with Power Conversion Efficiency of 7.4%. *Adv. Mater.* **2010**, *22*, E135−E138.

(31) Kim, J. B.; Allen, K.; Oh, S. J.; Lee, S.; Toney, M. F.; Kim, Y. S.; Kagan, C. R.; Nuckolls, C.; Loo, Y. L. Small-Molecule Thiophene-C_{60} Dyads As Compatibilizers in Inverted Polymer Solar Cells. *Chem. Mater.* **2010**, *22*, 5762−5773.

(32) Liang, Y. Y.; Yu, L. P. A New Class of Semiconducting Polymers for Bulk Heterojunction Solar Cells with Exceptionally High Performance. *Acc. Chem. Res.* **2010**, *43*, 1227−1236.

(33) Liu, C.; Mao, S.; Kuo, M. Cyanated Pentaceno[2,3-c]chalcogenophenes for Potential Application in Air-Stable Ambipolar Organic Thin-Film Transistors. *J. Phys. Chem. C* **2010**, *114*, 22316−22321.

(34) Birks, J. B. *Photophysics of Aromatic Molecules*; Wiley: New York, 1970.

(35) Angliker, H.; Rommel, E.; Wirz, J. Electronic Spectra of Hexacene in Solution (Ground State. Triplet State. Dication and Dianion). *Chem. Phys. Lett.* **1982**, *87*, 208−212.

(36) Minami, T.; Ito, S.; Nakano, M. Theoretical Study of Singlet Fission in Oligorylenes. *J. Phys. Chem. Lett.* **2012**, *3*, 2719−2723.

(37) Frisch, M. J.; et al. *Gaussian 09*, Revision A.1; Gaussian, Inc.: Wallingford, CT, 2009.

(38) Anthony, J. E.; Gierschner, J.; Landis, C. A.; Parkin, S. R.; Sherman, J. B.; Bakus, R. C. A New Functionalization Strategy for Pentacene. *Chem. Commun.* **2007**, 4746−4748.

(39) Vallett, P. J.; Snyder, J. L.; Damrauer, N. H. Tunable Electronic Coupling and Driving Force in Structurally Well Defined Tetracene Dimers for Molecular Singlet Fission: A Computational Exploration Using Density Functional Theory. *J. Phys. Chem. A* **2013**, *117*, 10824−10838.

(40) Minami, T.; Ito, S.; Nakano, M. Fundamental of Diradical-Character-Based Molecular Design for Singlet Fission. *J. Phys. Chem. Lett.* **2013**, *4*, 2133−2137.

(41) Ito, S.; Minami, T.; Nakano, M. Diradical Character Based Design for Singlet Fission of Condensed Ring Systems with 4nπ Electrons. *J. Phys. Chem. C* **2012**, *116*, 19729−19736.

(42) Coropceanu, V.; Kwon, O.; Wex, B.; Kaafarani, B. R.; Gruhn, N. E.; Durivage, J. C.; Neckers, D. C.; Brédas, J. Vibronic Coupling in Organic Semiconductors: The Case of Fused Polycyclic Benzene-Thiophene Structures. *Chem.—Eur. J.* **2006**, *12*, 2073−2080.

(43) Palayangoda, S. S.; Mondal, R.; Shah, B. K.; Neckers, D. C. Synthesis of Highly Soluble and Oxidatively Stable Tetraceno[2,3-b]thiophenes and Pentacenes. *J. Org. Chem.* **2007**, *72*, 6584−6587.

(44) Katz, H. E.; Bao, Z. The Physical Chemistry of Organic Field-Effect Transistors. *J. Phys. Chem. B* **2000**, *104*, 671−678.

(45) Laquindanum, J. G.; Katz, H. E.; Lovinger, A. J. Synthesis, Morphology, and Field-Effect Mobility of Anthradithiophenes. *J. Am. Chem. Soc.* **1998**, *120*, 664−672.

(46) Minami, T.; Nakano, M. Diradical Character View of Singlet Fission. *J. Phys. Chem. Lett.* **2012**, *3*, 145−150.

(47) Nakanoa, M.; Nakagawa, N.; Ohta, S.; Kishi, R.; Kubo, T.; Kamada, K.; Ohta, K.; Champagne, B.; Botek, E.; Takahashi, H.; Furukawa, S.; Morita, Y.; Nakasuji, K.; Yamaguchi, K. Second Hyperpolarizabilities of Polycyclic Diphenalenyl Radicals: Effects of Para/Ortho-Quinoid Structures and Central Ring Modification. *Chem. Phys. Lett.* **2006**, *429*, 174−179.

(48) Kishi, R.; Dennis, M.; Fukuda, K.; Murata, Y.; Morita, K.; Uenaka, H.; Nakano, M. Theoretical Study on the Electronic Structure and Third-Order Nonlinear Optical Properties of Open-Shell Quinoidal Oligothiophenes. *J. Phys. Chem. C* **2013**, *117*, 21498−21508.

(49) Cui, G.; Fang, W. Ab Initio Trajectory Surface-Hopping Study on Ultrafast Deactivation Process of Thiophene. *J. Phys. Chem. A* **2011**, *115*, 11544−11550.